

Visualization of focal sites of transcription within human nuclei

Dean A.Jackson, A.Bassim Hassan,
Rachel J.Errington¹ and Peter R.Cook

Sir William Dunn School of Pathology, University of Oxford, South Parks Road, Oxford OX1 3RE and ¹Department of Zoology, University of Oxford, South Parks Road, Oxford OX1 3PS, UK

Communicated by N.J.Proudfoot

HeLa cells were encapsulated in agarose microbeads, permeabilized and incubated with Br-UTP in a 'physiological' buffer; then sites of RNA synthesis were immunolabelled using an antibody that reacts with Br-RNA. After extending nascent RNA chains by <400 nucleotides *in vitro*, ~300–500 focal synthetic sites can be seen in each nucleus by fluorescence microscopy. Most foci also contain a component of the splicing apparatus detected by an anti-Sm antibody. α -amanitin, an inhibitor of RNA polymerase II, prevents incorporation into these foci; then, using a slightly higher salt concentration, ~25 nucleolar foci became clearly visible. Both nucleolar and extra-nucleolar foci remain after nucleolytic removal of ~90% chromatin. An underlying structure probably organizes groups of transcription units into 'factories' where transcripts are both synthesized and processed. **Key words:** nucleolus/nucleoskeleton/RNA polymerase I/RNA polymerase II/transcription foci

Introduction

Views on how the pathway involved in RNA processing is organized are evolving rapidly. Traditional views were based upon the often unstated assumption that relevant enzymes were freely diffusible: a soluble RNA polymerase would bind at a promoter and process along the DNA; then nascent RNA would be capped, methylated, spliced and polyadenylated by complexes formed from other soluble activities before the processed transcripts diffused through nuclear pores to the cytoplasm. According to this simplified view, sites of synthesis and processing would be spread throughout nuclei, reflecting the concentration of active chromatin.

Recent studies point to a more structured pathway (reviewed by Spector, 1990; Carter *et al.*, 1991; Jackson, 1991). Various components of the spliceosome, caps, nascent RNA and poly(A) are concentrated in nuclear 'speckles' detected with the appropriate antibodies (Fu and Maniatis, 1990; Carmo-Fonseca *et al.*, 1991a,b; Carter *et al.*, 1991; Huang and Spector, 1991; Elliot *et al.*, 1992). Moreover, specific transcripts are not diffusely spread but concentrated on curvilinear 'tracks' connecting genes to the periphery (Lawrence *et al.*, 1989; Xing and Lawrence 1991). Such observations suggest that transcripts are processed on, and transported along, an underlying solid phase.

Visualizing sites of RNA synthesis poses special problems. Analysis *in vivo* is difficult because transcription occurs so

rapidly (i.e. ~1400 nucleotides/min; Shermoen and O'Farrell, 1991) that labelling for even a minute or two allows ample time for completed transcripts to travel far from the synthetic site; then, label marks not the synthetic site, but a site of accumulation later in the pathway. Transcription *in vitro* at a reduced rate permits labelling of synthetic sites, but *in vitro* studies are bedevilled by the problem of artefacts. Thus, studies on 'nucleoids' isolated in 2 M NaCl first suggested that active RNA polymerases might be fixed to a solid phase (Jackson *et al.*, 1981, 1984) but the associations seen could have been created artefactually. Unphysiological salt concentrations are used when isolating nuclear derivatives like 'nucleoids', 'matrices' and 'scaffolds' because chromatin aggregates at an isotonic salt concentration (Cook, 1988). This problem can be side-stepped by encapsulating cells in agarose microbeads ($r = \sim 25 \mu\text{m}$) before lysing membranes in a 'physiological' buffer (Jackson *et al.*, 1988). Such encapsulated nuclei can be pipetted freely; they are protected by the agarose yet accessible to molecular probes. As they continue to transcribe at essentially the rate found *in vivo*, it seems unlikely that active polymerases or nascent RNA could then have aggregated artefactually.

We have now immunolocalized sites of RNA synthesis *in vitro* using such encapsulated nuclei; we find several hundred focal sites scattered throughout nuclei. Each site must contain many polymerases. The sites remain even when most chromatin is removed, presumably because they are attached to a solid phase.

Results

Incorporation of Br-UTP by permeabilized cells

We first established conditions necessary to label sites of synthesis using analogues that could be detected by immunofluorescence after incorporation into RNA (i.e. Br-UTP, biotin-11-UTP and digoxigenin-11-UTP). After permeabilizing plasma membranes with streptolysin O, encapsulated HeLa cells continue to elongate nascent RNA chains efficiently under optimal conditions (Jackson *et al.*, 1988; not shown); here we deliberately use inefficient conditions to ensure that synthetic sites are labelled, rather than distant processing sites.

Using a limiting concentration of GTP with [³²P]GTP as a tracer, Br-UTP was incorporated more efficiently than biotin-11-UTP or digoxigenin-11-UTP into acid-insoluble material (Figure 1A, compare curve 2 with curves 3 and 4). When the GTP concentration was increased to 100 μM , incorporation of Br-UTP increased to a level that allowed detection of incorporated Br by immunolabelling (Figure 1B, curve 2). Assuming there are ~35 000 active RNA polymerases per cell (not shown; Cox, 1976), each nascent RNA chain is initially elongated at 40 nucleotides/min using our standard conditions. As >95% nascent RNA chains are >400 nucleotides long (Naora, 1977; not shown), essentially all Br-UTP will be incorporated during 10 min into growing

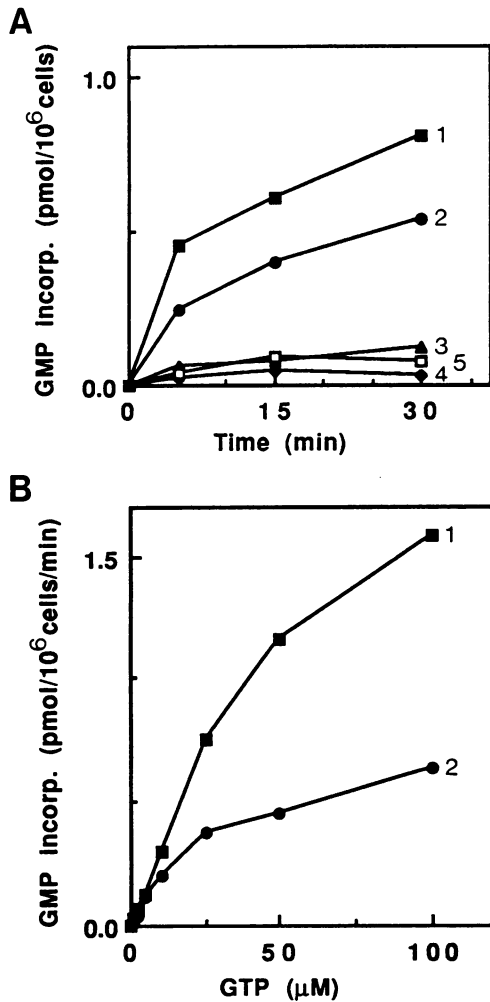


Fig. 1. Effects of various analogues on transcription rates. (A) Transcription rates (measured by incorporation of [³²P]GTP into acid-insoluble material) in the presence of (1) 100 μM UTP, (2) 100 μM Br-UTP, (3) 100 μM biotin-11-UTP, (4) 10 μM digoxigenin-11-UTP and (5) without UTP or its analogues. (B) Transcription rates of unencapsulated and permeabilized cells with 100 μM UTP (curve 1) or Br-UTP (curve 2) and various concentrations of GTP.

chains that remain attached to polymerization sites. [Note that although ~10% nuclear RNA is only 80–260 nucleotides long, it is stable and constitutes a very minor proportion of nascent RNA (Naora, 1977).] α -amanitin, an inhibitor of RNA polymerase II, reduces incorporation to 17%; most of the remaining synthesis is due to polymerase I (not shown).

Visualization of sites of transcription

Cells were encapsulated, lysed with streptolysin and incubated for different times with Br-UTP. After permeabilizing the nuclear membrane with Triton and fixation, sites of incorporation were indirectly immunolabelled using an antibody that reacts with Br-RNA, followed by a second antibody conjugated with Texas red. Faintly fluorescing foci formed a network spreading throughout extra-nucleolar regions (Figure 2A). As the incorporation time increases, the overall fluorescence increases (Figure 2A–D). Foci do not coincide with local concentrations of DNA detected by

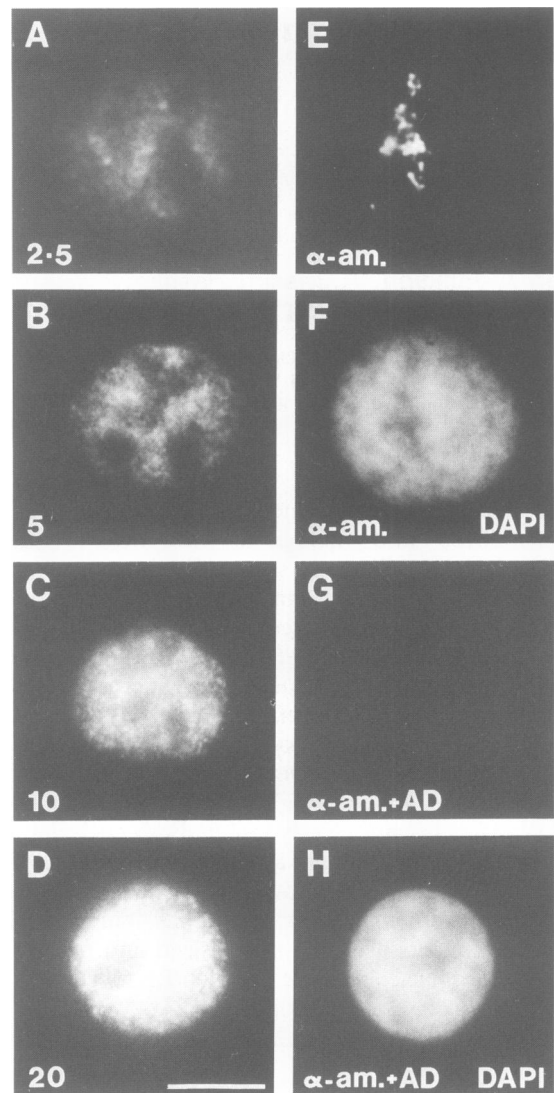


Fig. 2. Sites of transcription labelled by indirect immunofluorescence. Bar: 5 μm. (A–D): encapsulated cells were lysed with streptolysin, incubated with Br-UTP for (A) 2.5, (B) 5, (C) 10 or (D) 20 min and sites of incorporation labelled (first antibody: mouse anti-Br-RNA; second antibody: anti-mouse, Texas red-conjugated). (E and F): As (C) except 50 mM NH₄SO₄ and α -amanitin (α -am) were present during incorporation. (E) Texas red fluorescence. (F) DAPI fluorescence of cell in E. (G and H) As (E and F) except actinomycin D (AD) was also present. (G) Texas red fluorescence; (H) DAPI fluorescence of cell in G.

DAPI (4',6'-diamidino-2-phenylindole; see later). Controls described in Materials and methods show that only sites containing Br-RNA are labelled.

Figure 2 panels A–D represent round nuclei, so many foci lie above and below the focal plane, generating an out-of-focus 'flare'; individual foci are then best seen at the periphery. The use of a confocal laser scanning microscope ('confocal' microscope) enables optical sectioning and removal of out-of-focus flare. Discrete foci become clearly visible, both in a single slice (Figure 3A and C; SI) and when six separate slices taken through one nucleus are projected on to a plane (Figure 3B and D; Proj). Inspection shows there to be ~300–500 foci/nucleus in these aneuploid cells.

Images seen by conventional or confocal microscopy after incubation for <2.5 min with Br-UTP are very faint (not

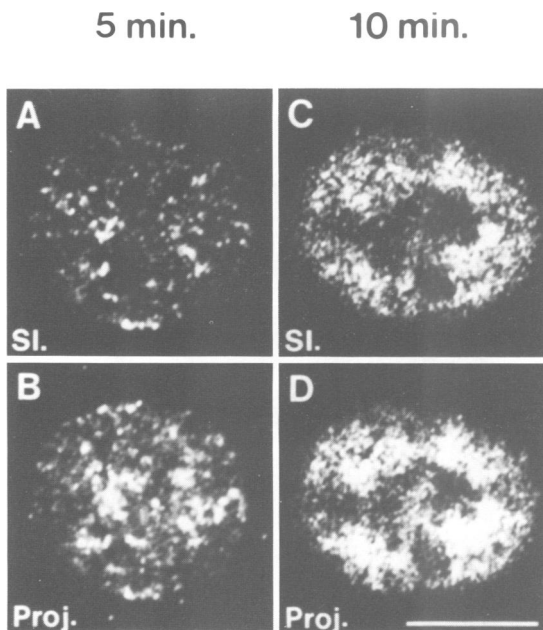


Fig. 3. Sites of transcription visualized by confocal microscopy. Encapsulated and permeabilized cells were incubated with Br-UTP for (A) 5 or (C) 10 min and sites of incorporation labelled as in Figure 2. In each case, nine optical slices were taken through a nucleus. Top panels: a central slice (SI). Bottom panels: maximum projection (Proj) of all sections on to a single plane. Bar: 5 μ m.

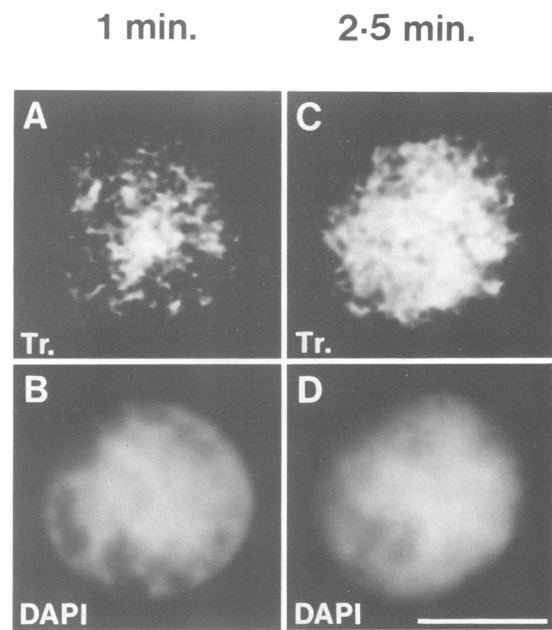


Fig. 4. Sites of transcription visualized using a CCD camera. Encapsulated and permeabilized cells were incubated with Br-UTP for (A) 1 or (C) 2.5 min, sites of incorporation labelled as in Figure 2, and images captured. Top panels: Texas red fluorescence labelling transcription foci (Tr). Bottom panels: DAPI-fluorescence of cell shown above. Bar: 5 μ m.

shown). The use of a charge coupled device (CCD) as a camera allows imaging after shorter incubations; however, the device must be used carefully as images can be distorted by digital manipulation (e.g. background subtraction and grey-scale manipulation). Therefore we deliberately captured the primary image using a single 2 s exposure with zero gain and processed it minimally (i.e. the image was median filtered and linearly contrast extended to fill the 256 pixel grey-scale); no other background was subtracted, nor were several exposures integrated over time or space. The resulting images are views of whole cells against a 'real' background, including out-of-focus flare; they are roughly comparable to those obtained by conventional photography.

After 1 min incorporation, a speckled network reminiscent of that seen by conventional photography after 5 min is visible (compare Figure 4A with Figure 2B); again the network does not coincide with high DNA concentrations (Figure 4A and B; DAPI staining is uniform throughout extra-nucleolar regions). After 2.5 min incorporation, the pattern resembles that seen after 10 min by conventional photography (compare Figure 4C with Figure 2C). Clearly, increased sensitivity allows detection of similar patterns after shorter incorporations.

Nucleolar foci

After short incorporations using our standard conditions, nucleoli do not generally contain foci detectable by conventional microscopy and appear as black 'holes' (Figure 2A–C); GC-rich rRNA labels poorly with Br-UTP. Overall transcription rates (measured using labelled GTP) can be increased 1.9 times, and polymerase I rates 4 times, by adding 50 mM NH_4SO_4 to the 'physiological' buffer (not shown; see also Jackson and Cook, 1985a). Then discrete nucleolar foci become visible. If α -amanitin is also

used to inhibit incorporation into extra-nucleolar regions, the large nucleolar foci become quite obvious (Figure 2E and F; nucleoli stain weakly, if at all, with DAPI and what staining there is results from out-of-focus flare). There are variable numbers of such foci in these aneuploid cells, with an average of 23 ± 5 foci/nucleus ($n = 50$; range 16–37). They often appear clustered as if strung along an underlying thread (Figure 2E). Addition of both α -amanitin and actinomycin D (at a concentration sufficient to inhibit polymerase I) eliminates all incorporation (Figure 2G and H). [Note that the unphysiologically high salt concentration increases activity; artefactual aggregation might be expected to reduce it. Note also that after lysis with Triton (rather than streptolysin O) and using our standard 'physiological' conditions, nucleolar foci can be seen after 10 min incorporation; then the intensity of the extra-nucleolar foci is also slightly reduced (not shown).]

Extra-nucleolar foci contain snRNPs

The relationship of extra-nucleolar transcription sites to nuclear 'speckles' reactive with anti-Sm antibodies (i.e. containing small nuclear ribonucleoproteins or snRNPs) was determined by double-labelling. Figure 5 illustrates four optical sections taken at 1 μ m intervals through one typical nucleus using a 'confocal' microscope. Ratios of fluorescence due to Br- and Sm-labelling are displayed as pseudo-colours (bar), ranging from blue (100% Br-RNA, 0% Sm antigen) to red (0% Br-RNA, 100% Sm antigen). Most Sm antigens are found at transcription sites, giving an intermediate yellow colour. Some transcription sites are devoid of Sm antigen and appear blue, whilst few concentrations of Sm antigen contain no Br-RNA and appear red. Whilst these results qualitatively indicate that transcription sites are heterogeneous with respect to Sm content, the relative efficiencies

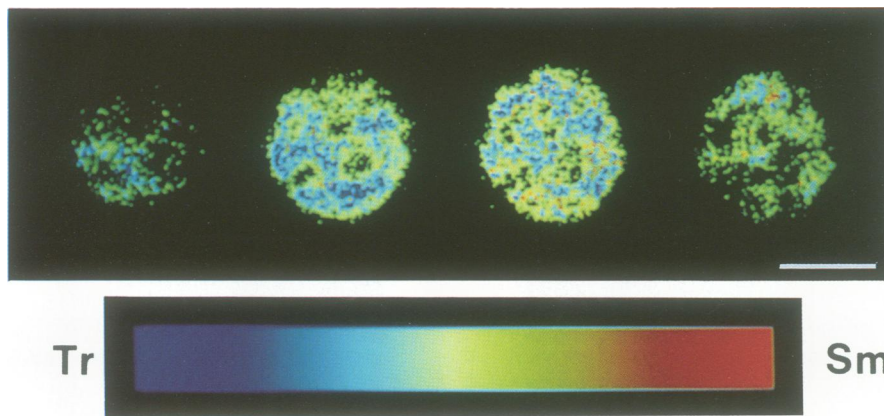


Fig. 5. Colocalization by confocal microscopy of transcription sites and concentrations of Sm antigens. Encapsulated and permeabilized cells were incubated with Br-UTP for 10 min and sites containing Sm antigens and Br-RNA were doubly labelled. Four optical sections were taken at 1 μ m intervals through the centre of one nucleus. The pseudo-colour display illustrates relative fluorescence, ranging from 100% Br-RNA, 0% Sm antigen (Tr; blue) to 0% Br-RNA, 100% Sm antigen (red). Most Sm antigens colocalize with transcription sites and so appear yellow; some transcription sites are devoid of Sm antigen and appear blue. Bar: 5 μ m.

with which transcription sites and Sm antigens are detected is unknown; therefore accurate quantification awaits further study.

Many transcription foci are distinct from replication foci seen late during S-phase

About 150 sites of incorporation of biotin-11-dUTP into DNA have been visualized in tissue culture cells; these replication sites change in intensity and shape as cells progress through S-phase (Nakayasu and Berezney, 1989). In order to confirm that Br-UTP was not labelling replication sites, it was important to show that sites of incorporation of Br-UTP and biotin-11-dUTP were distinct. However, the changes in number and shape of replication foci during S-phase—and their relationship with transcription foci—is complicated (A.Bassim Hassan, Dean A.Jackson, Rachel Errington and Peter R.Cook; in preparation); here we demonstrate only that most transcription sites differ from replication sites late in S-phase.

Unsynchronized cells were encapsulated, permeabilized and incubated with both analogues; then sites of incorporation were indirectly immunolabelled and viewed in a 'confocal' microscope. Most cells in the population were labelled with anti-Br-RNA antibodies to give patterns like those in Figure 3. In contrast, ~25% were labelled with FITC-streptavidin, giving patterns typical of S-phase cells (Nakamura *et al.*, 1986; Nakayasu and Berezney, 1989). Figure 6 illustrates a section through one late S-phase nucleus; most transcription sites are clearly distinct from replication sites. There is no cross-labelling or 'bleed-through' between the different channels used for double-labelling with FITC and Texas red.

Both nucleolar and extra-nucleolar foci resist electroelution

Both RNA polymerase I and II activities, as well as nascent RNA, resist electroelution even when most chromatin is removed (Jackson and Cook, 1985b; Jackson *et al.*, 1988; Dickinson *et al.*, 1990); therefore we would also expect transcription foci to resist elution. Permeabilized cells were incubated for 10 min with Br-UTP and treated with nucleases to fragment chromatin into ~10 kbp pieces; then ~90% chromatin was electroeluted and transcription sites were

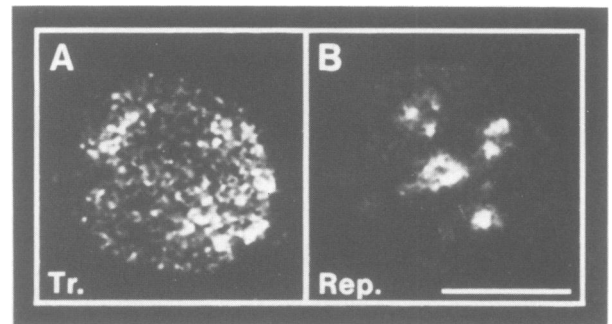


Fig. 6. Colocalization by confocal microscopy of sites of replication and transcription. Encapsulated and permeabilized cells were incubated with Br-UTP and biotin-11-dUTP for 10 min and sites of transcription (A; Tr) and replication (B; Rep) labelled with Texas red and FITC respectively. Bar: 5 μ m.

immunolabelled. There is, of course, cell-to-cell variation in the amount of chromatin remaining after elution and so typical examples are illustrated. Both nucleolar and extra-nucleolar foci resist elution, despite removal of most chromatin (as indicated by faint DAPI staining; Figure 7).

Discussion

Transcription foci

Transcription sites were visualized by incubating encapsulated and permeabilized HeLa cells with Br-UTP in a 'physiological' buffer; then sites containing nascent Br-RNA were indirectly immunolabelled. This approach has several advantages. First, the transcription rate can be adjusted to ~40 nucleotides/min (Figure 1) so that during short pulses polymerization sites—rather than distant processing or storage sites—will be labelled. [After 10 min incorporation *in vivo*, >95% transcripts are >400 nucleotides long (Naora, 1977; not shown).] Secondly, the encapsulating agarose permits thorough washing and so low backgrounds, whilst preserving structure. Thirdly, the use of 'physiological' conditions and retention, under optimal conditions, of most transcriptional activity of the living cell up to fixation provides some assurance that the polymerizing sites analysed are not generated artefactually.

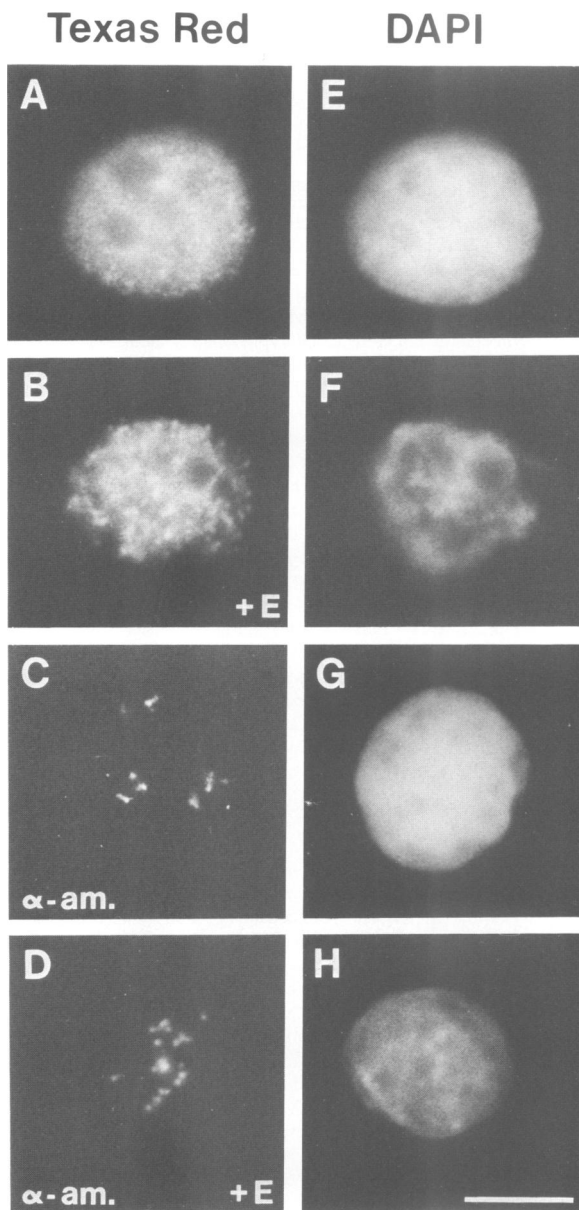


Fig. 7. Transcription sites resist electroelution. Encapsulated cells in early S-phase were lysed with streptolysin, incubated with Br-UTP for 10 min, treated with Triton and (B) 90 or (D) 93% chromatin eluted from some beads (indicated by +E); then sites of incorporation were indirectly immunolabelled as in Figure 2. (C and D) α -amanitin (α -am) present during incorporation. Left: Texas red fluorescence. Right: DAPI-staining of cell on left. Bar: 5 μ m.

RNA polymerases I and II are responsible for most nucleolar and extra-nucleolar transcription respectively. Our results show that transcription sites in both regions are not diffusely spread, reflecting the distribution of DNA; rather, they are focally concentrated (Figures 2–4). The sites are distinct from replication foci seen late during S-phase (Figure 6).

Wansink, D.G., Schul, W., van der Kraan, I., van Steensel, B., van Driel, R. and de Jong, L. (submitted) have recently visualized similar foci after microinjection of Br-UTP into cells. Their results neatly complement ours. The long incubations used *in vivo* make it impossible to be certain that transcripts have not left their synthetic site to accumulate elsewhere, whilst our *in vitro* experiments cannot completely

exclude the possibility that foci are aggregation artefacts. The combined results make it likely that both sets of foci reflect the same, natural, synthetic sites.

Polymerase I foci

Precisely where active RNA polymerase I is within nucleoli is controversial; one possibility is that it is concentrated in local regions (Scheer and Rose, 1984; reviewed by Jordan, 1991 and Fischer *et al.*, 1991). When extra-nucleolar transcription is inhibited and nucleolar transcription stimulated, we see ~25 discrete nucleolar foci (Figure 2E). As HeLa cells contain ~500 ribosomal cistrons (Schmickel, 1973), of which ~150 are active (Davis *et al.*, 1983; Dickinson *et al.*, 1990; Haaf *et al.*, 1991), each focus must contain about six active transcription units, each with ~100 polymerases spaced every ~100 bp (Miller and Bakken, 1972).

Transcription factories containing polymerase II

Extra-nucleolar (polymerase II) foci react with an anti-Sm antibody commonly used to label snRNPs, and so spliceosomes (Figure 5). Although the antibody detects concentrations of Sm antigens, rather than sites of activity, it is nevertheless attractive to suppose that these foci are transcription 'factories' where RNA is both made and processed. They would be analogous to the replication factories seen recently (Hozák, P., Hassan, A.B., Jackson, D.A. and Cook, P.R.). Various other extra-nucleolar structures have been detected—including nuclear 'bodies' (Vagner-Capodano *et al.*, 1982; Fusconi *et al.*, 1991), 'dots' (Ascoli and Maul, 1991), 'coiled bodies' (Raska *et al.*, 1991) and 'polymorphic interphase karyosomal associations' (PIKAs; Saunders *et al.*, 1991)—but none of these have been shown to be transcriptionally active. When living cells are incubated with [³H]uridine for short periods, label becomes associated with perichromatin fibrils close to condensed chromatin (reviewed by Fakan and Puvion, 1980), but it is not clear whether these represent sites of synthesis or sites where transcripts accumulate. Carter *et al.* (1991) have also visualized ~20 domains rich in poly(A) that they suggest may be synthetic sites but these, too, could equally be sites of accumulation.

It is difficult to estimate accurately the total number of these foci, because they are so variable in intensity and size, close to the resolution afforded by light microscopy. Although we can only see ~300–500, it is possible—though unlikely—that there are many more below the level of detection. Consider an extreme case in which ~25 000 polymerase II molecules (Cox, 1976; not shown) are in transcription units randomly distributed throughout euchromatin; this inevitably means that there will be local variations in concentration, which—if above a critical threshold—will be detected. By judicious choice of threshold, number of polymerases per transcription unit and volume occupied by nascent RNA, simulations show that such random distributions can appear as apparently discrete foci (not shown). Several reasons make this explanation unlikely. First, intensity profiles across such randomly generated foci rise and fall gently. However, profiles across foci at the edge of nuclei in Figure 4 rise over a pixel or two to a plateau and fall equally precipitously (not shown). Secondly, about equal numbers of discrete foci are imaged using conventional photography, a CCD camera and confocal microscopy; if transcription units were randomly distributed, we should

detect more foci using the more sensitive CCD camera. Thirdly, a rough comparison of the number and intensity of the different foci makes it likely that most are detected. Nucleolar foci contain ~600 active polymerases (see above); although variable in intensity, many extra-nucleolar foci are ~1/5 as bright and so would contain ~120 active polymerases if they incorporated as efficiently. However, Br-UTP labels the GC-rich ribosomal transcripts poorly, so each extra-nucleolar focus probably contains ~60 active enzymes. Then we can account for 24 000 of the 25 000 active polymerases in 400 foci. [Note that these calculations are inevitably very rough.]

A fourth reason is more decisive. We have visualized replication sites using the same equipment, with the same background settings (Figure 6B; Hozák, P., Hassan, A.B., Jackson, D.A. and Cook, P.R., submitted). Transcription foci prove roughly similar to the replication foci of early S-phase which are uniformly distributed, unlike the clusters seen later (Figure 6B; there are about twice as many transcription foci as replication foci and they vary more in intensity). Electron microscopy confirms that most active DNA polymerizing activity is contained in discrete foci, with little if any activity outside them (Hozák, P., Hassan, A.B., Jackson, D.A. and Cook, P.R., submitted). As intensity profiles across individual replication and transcription foci have similarly sharp cut-offs (not shown), it seems likely that the transcription sites will be equally discrete.

These results, then, are most simply interpreted if there are, indeed, only 300–500 polymerase II sites/nucleus, with each containing many active genes and ~60 polymerases. However, decisive proof must await precise morphometric analysis at the ultrastructural level.

Attachment of transcription foci to a solid phase

Presumably some underlying structure organizes many transcription units into these foci. Both types appear to be strung along an invisible skeleton (Figures 2–4) and their failure to elute with most chromatin (Figure 7) confirms that nascent RNA is attached to some large structure. Candidate skeletons include the ~4 nm and intermediate filaments seen in nucleolar and extra-nucleolar regions respectively (Franke *et al.*, 1981; Jackson and Cook, 1988; He *et al.*, 1990). But whether an underlying skeleton exists—and whether active polymerases and nascent RNA are attached to it—is also controversial (Cook, 1988, 1989; Dickinson *et al.*, 1990). It is now possible to extend these studies to the ultrastructural level to establish whether sites of incorporation—and so active polymerases—are associated with a solid phase.

Materials and methods

Encapsulation and lysis

Suspension cultures of HeLa cells were grown in minimal essential medium supplemented with 5% fetal calf serum. Cells were washed three times in PBS and encapsulated (2×10^6) in 0.5% agarose (Jackson *et al.*, 1988). Encapsulated cells were incubated with streptolysin O (Sigma; 1000 units/ml/ 10^6 cells; 30 min; 4°C) in an equal volume of ice-cold PBS, washed first with 10 vol ice-cold PBS to remove unbound streptolysin and then 'physiological' buffer (PB). [PB (pH 7.4) contains 22 mM Na⁺, 130 mM K⁺, 1 mM Mg²⁺, <0.3 μM free Ca²⁺, 31 mM Cl⁻, 100 mM acetate, 11 mM phosphate, 1 mM ATP, 1 mM dithiothreitol and 0.2 mM phenylmethylsulfonyl fluoride (PMSF) (modified from Jackson *et al.*, 1988; 130 mM KCl is replaced by 100 mM CH₃COOK and 30 mM KCl).] Beads were resuspended in an equal volume of PB and immediately permeabilized by incubation (3 min) at 37°C. >90% plasma membranes were

permeabilized (monitored using trypan blue) but nuclear membranes remained intact (i.e. excluded mouse FITC-IgG; Amersham).

All solutions used were treated with diethylpyrocarbonate to eliminate RNases (Sambrook *et al.*, 1989). In addition, RNasin was added during incubations with antibodies, subsequent washes and electroelution to final concentrations of 25, 2.5 and 0.25 units/ml respectively.

Transcription in vitro

Encapsulated and permeabilized cells in PB were pre-incubated (33°C; 2 min; note that there is no thermally induced chromatin aggregation at 33°C; Jackson *et al.*, 1988), and prewarmed transcription mix (10× concentrate) added to give final concentrations of 2 mM ATP, 0.1 mM CTP, GTP and UTP (or Br-UTP; Sigma) and 2 mM MgCl₂. In most cases 0.01 mM TTP and 5 μg/ml aphidicolin were added to prevent any incorporation by DNA polymerases; this had no visible effect on foci. Reactions were incubated at 33°C and stopped by adding 10 vol ice-cold PB. After pelleting and repeating the wash in ice-cold PB, nuclei were immediately permeabilized by incubation (10 min; 4°C) in 10 vol 0.2% Triton X-100 in PB, followed by three further washes in ice-cold PB before fixation. If added, α-amanitin (10–100 μg/ml) and/or actinomycin D (0.2 μg/ml) were present for 10 min at 4°C prior to, and during, transcription.

For Figure 1A, standard conditions were used except that UTP was omitted, GTP reduced to 2 μM, [³²P]GTP added (Amersham; 3000 Ci/mmol; 20 μCi/ml) and UTP or its analogues added as shown; for the experiment shown in Figure 1B, unencapsulated cells were used with 100 μM UTP or Br-UTP, plus variable amounts of GTP and [³²P]GTP (10–500 μCi/ml). ³²P incorporation into acid-insoluble material was measured by scintillation counting (Jackson and Cook, 1986a). For Figure 6, prewarmed initiation mix (10× concentrate) was added to permeabilized and encapsulated cells to give final concentrations of 2 mM ATP, 0.1 mM CTP, GTP and Br-UTP, 0.1 mM dATP, dCTP, dGTP and biotin-11-dUTP (Sigma) and 2 mM MgCl₂; after 10 min incubation, reactions were stopped as above.

Immunolabelling

After transcription reactions, cells were fixed (15 min; 4°C) in fresh 4% paraformaldehyde in PB, washed twice in PB and twice in PBS supplemented with 0.05% Tween 20 (Sigma). Sites containing Br-RNA were then indirectly immunolabelled using a primary antibody raised against a bromodeoxyuridine–BSA conjugate (i.e. anti-bromodeoxyuridine; mouse monoclonal IgG; Boehringer; 2 μg/ml) which cross-reacts with Br-RNA. Various controls demonstrated that this antibody reacted with Br-RNA and not Br-DNA. No labelling was seen if Br-UTP was replaced with 100 μM UTP during transcription or if the first antibody was omitted. If 50 μg/ml α-amanitin was present prior to, and during, transcription, extra-nucleolar labelling was abolished; addition of 0.2 μg/ml actinomycin D also abolished nucleolar labelling. Labelled foci were also removed by treatment (15 min; 35°C) with pancreatic RNase (25 U/ml)—but not DNase I (5.8 U/ml; 50 μg/ml; RNase-free)—prior to immunolabelling (see also Jackson and Cook, 1985b, 1986b). The experiment described in Figure 6 also shows there is no cross-labelling or 'bleed-through' between the different channels used to detect FITC and Texas red.

Beads were incubated (4 h; 4°C) with primary antibody, washed four times in PBS + Tween, incubated (16 h; 4°C) with secondary antibody (sheep anti-mouse IgG, Texas Red-conjugated; Amersham; 1/500 dilution) and BSA (0.5%), washed four times in PBS + Tween, then twice in PBS and then mounted under coverslips in Mowiol 4–88 (Hoechst) containing 0.1 μg/ml DAPI (Boehringer) and 2.5% DABCO (1,4-diazobicyclo-[2.2.2]-octane; Sigma). For Figure 5, beads were incubated (2 h; 4°C) with anti-Sm (anti-nuclear antigen reference human serum #5; Center for Disease Control, Atlanta; 1/50 000 dilution), washed, then incubated (2 h; 4°C) with FITC-conjugated goat anti-human IgG (Sigma; 1/2000 dilution), rewashed and treated with anti-bromodeoxyuridine and then the sheep anti-mouse IgG as above. For Figure 6, streptavidin-FITC (Sigma; 0.5 pg/ml) was included with the second antibody.

Microscopy

Photographs were taken using a Zeiss Axiophot microscope (100× oil-immersion objective; NA 1.3; 'Optivar' setting, 1.25; filter sets: 2, 9 and 14) and Tmax black and white film, push-processed to ASA 1600 (20–40 and 2–10 s exposures for fluorescent antibodies and DAPI respectively). Images were also captured with a Hamamatsu (1000×1018 pixel) CCD (Peltier-cooled; –40°C) attached to the Axiophot and processed using Prism software on a MacIntosh Quadra.

Labelled cells were also examined using a Bio-Rad MRC 600 laser-scanning confocal microscope attached to a Nikon Diaphot inverted microscope with an oil-immersion objective (60×; NA 1.4). Simultaneous

3D (x,y,z) images were acquired, using an argon-ion laser (wavelength, 514 nm) of cells double-labelled with a FITC (Sm antigen) and Texas red (Br-RNA) probe. A typical image consisted of eight 1 μ m optical sections/cell. These were projected onto a single plane using a maximum brightness algorithm (Figure 3). The relative distribution of the two fluorochromes for each optical slice was analysed by calculating the emission ratio. A threshold operation was applied to remove background, before assigning a pseudo-colour map. Bright regions of output indicate areas of high original intensity and are hence more reliable (i.e. bright red, yellow and blue).

Digestion and electroelution

Cells were labelled (22 h) with [methyl-³H]thymidine (0.05 μ Ci/ml; 60 Ci/mmol) to label DNA uniformly, and were then encapsulated, permeabilized, labelled with Br-UTP and washed free of precursors. Then beads were incubated (15 min; 33°C) with *Eco*RI (2500 U/ml) and *Hae*III (500 U/ml) in PB to cut chromatin into ~10 kb pieces (*Eco*RI cuts a *Hae*III-resistant satellite). Finally ~90% chromatin was removed (measured by removal of ³H; Jackson *et al.*, 1990) by electrophoresis (0.8% agarose gel; 4 V/cm; 4 h; Jackson *et al.*, 1988) in PB supplemented with PMSF.

Acknowledgements

We thank the Cancer Research Campaign (P.R.C and D.A.J.), the Wellcome Trust (A.B.H) and the Medical Research Council (R.E) for support. David Shotton kindly allowed us to use the confocal microscope, and Nick White and David Vaux helped us greatly with it.

References

- Ascoli, C. and Maul, G. (1991) *J. Cell Biol.*, **112**, 785–795.
- Carmo-Fonseca, M., Tollervey, D., Pepperkok, R., Barabino, S.M.L., Merdes, A., Brunner, C., Zamore, P.D., Green, M.R., Hurt, E. and Lamond, A.I. (1991a) *EMBO J.*, **10**, 195–206.
- Carmo-Fonseca, M., Pepperkok, R., Sproat, B.S., Ansorge, W., Swanson, M.S. and Lamond, A.I. (1991b) *EMBO J.*, **10**, 1863–1873.
- Carter, K.C., Taneja, K.L. and Lawrence, J.B. (1991) *J. Cell Biol.*, **115**, 1191–1202.
- Cook, P.R. (1988) *J. Cell Sci.*, **90**, 1–6.
- Cook, P.R. (1989) *Eur. J. Biochem.*, **185**, 487–501.
- Cox, R.F. (1976) *Cell*, **7**, 455–465.
- Davis, A.H., Reudelhuber, T.L. and Garrard, W.T. (1983) *J. Mol. Biol.*, **167**, 133–155.
- Dickinson, P., Cook, P.R. and Jackson, D.A. (1990) *EMBO J.*, **9**, 2207–2214.
- Elliot, D.J., Bowman, D.S., Abovich, N., Fay, F.S. and Rosbash, M. (1992) *EMBO J.*, **11**, 3731–3736.
- Fakan, S. and Puvion, E. (1980) *Int. Rev. Cytol.*, **65**, 255–299.
- Fischer, D., Weisenberger, D. and Scheer, U. (1991) *Chromosoma*, **101**, 133–140.
- Franke, W.W., Kleinschmidt, J.A., Spring, H., Krohne, G., Grund, C., Trendelenburg, M.F., Stoehr, M. and Scheer, U. (1981) *J. Cell Biol.*, **90**, 289–299.
- Fu, X.-D. and Maniatis, T. (1990) *Nature*, **343**, 437–444.
- Fusconi, M., Cassani, F., Govoni, M., Caselli, A., Farabegoli, F., Lenzi, M., Ballardini, G., Zauli, D. and Bianchi, F.B. (1991) *Clin. Exp. Immunol.*, **83**, 291–297.
- Haaf, T., Hayman, D.L. and Schmid, M. (1991) *Exp. Cell Res.*, **193**, 78–86.
- He, D., Nickerson, J.A. and Penman, S. (1990) *J. Cell Biol.*, **110**, 569–580.
- Huang, S. and Spector, D.L. (1991) *Genes Dev.*, **5**, 2288–2302.
- Jackson, D.A. (1991) *BioEssays*, **13**, 1–10.
- Jackson, D.A. and Cook, P.R. (1985a) *EMBO J.*, **4**, 913–918.
- Jackson, D.A. and Cook, P.R. (1985b) *EMBO J.*, **4**, 919–925.
- Jackson, D.A. and Cook, P.R. (1986a) *EMBO J.*, **5**, 1403–1410.
- Jackson, D.A. and Cook, P.R. (1986b) *J. Mol. Biol.*, **192**, 65–76.
- Jackson, D.A. and Cook, P.R. (1988) *EMBO J.*, **7**, 3667–3677.
- Jackson, D.A., Dickinson, P. and Cook, P.R. (1990) *EMBO J.*, **9**, 567–571.
- Jackson, D.A., McCreedy, S.J. and Cook, P.R. (1981) *Nature*, **292**, 552–555.
- Jackson, D.A., McCreedy, S.J. and Cook, P.R. (1984) *J. Cell Sci. Suppl.*, **1**, 59–79.
- Jackson, D.A., Yuan, J. and Cook, P.R. (1988) *J. Cell Sci.*, **90**, 365–378.
- Jordan, E.G. (1991) *J. Cell Sci.*, **98**, 437–442.
- Lawrence, J.B., Singer, R.H. and Marselle, L.M. (1989) *Cell*, **57**, 493–502.
- Miller, O.L. and Bakken, A.H. (1972) *Acta Endocrinol. (Suppl)*, **168**, 155–73.
- Nakamura, H., Morita, T. and Sato, C. (1986) *Exp. Cell Res.*, **165**, 291–297.
- Nakayasu, H. and Berezney, R. (1989) *J. Cell Biol.*, **108**, 1–11.
- Naora, H. (1977) In Stewart, P.R. and Letham, D.D. (eds), *The Ribonucleic Acids*, 2nd edition. Springer-Verlag, Berlin, pp. 43–80.
- Raska, I., Andrade, L.E.C., Ochs, R.L., Chan, E.K.L., Chang, C.-M., Roos, G. and Tan, E.M. (1991) *Exp. Cell Res.*, **195**, 27–37.
- Sambrook, J., Fritsch, E.F. and Maniatis, T. (1989) *Molecular Cloning. A Laboratory Manual*, 2nd edition. Cold Spring Harbor Laboratory Press, Cold Spring Harbor, NY.
- Saunders, W.S., Cooke, C.A. and Earnshaw, W.C. (1991) *J. Cell Biol.*, **115**, 919–932.
- Scheer, U. and Rose, K.M. (1984) *Proc. Natl. Acad. Sci. USA*, **81**, 1431–1435.
- Schmickel, R.D. (1973) *Pediat. Res.*, **7**, 5–12.
- Shermoen, A.W. and O'Farrell, P.H. (1991) *Cell*, **67**, 303–310.
- Spector, D.L. (1990) *Proc. Natl. Acad. Sci. USA*, **87**, 147–151.
- Vagner-Capodano, A.M., Bouteille, M., Stahl, A. and Lissitzky, S. (1982) *J. Ultrastruct. Res.*, **78**, 13–25.
- Xing, Y. and Lawrence, J.B. (1991) *J. Cell Biol.*, **112**, 1055–1063.

Received on October 20, 1992; revised on December 7, 1992